JACS
JOURNAL OF THE AMERICAN CHEMICAL SOCIETY
Communication
pubs.acs.org/JACS

# Spectroscopic Characterization of the Bridging Amine in the Active Site of [FeFe] Hydrogenase Using Isotopologues of the H-Cluster

Agnieszka Adamska-Venkatesh,[†] Souvik Roy,[‡] Judith F. Siebel,[†] Trevor R. Simmons,[‡,∥] Marc Fontecave,[‡,§] Vincent Artero,[‡] Edward Reijerse,*[,†] and Wolfgang Lubitz*[,†]

[†]Max-Planck-Institut für Chemische Energiekonversion, Stiftstrasse 34-36, 45470 Mülheim an der Ruhr, Germany

[‡]Laboratoire de Chimie et Biologie des Métaux, Université Grenoble Alpes, CEA, CNRS, 17 rue des martyrs, 38000 Grenoble, France

[§]Laboratoire de Chimie des Processus Biologiques, Collège de France, Université Pierre et Marie Curie, CNRS UMR 8229, 11 place Marcelin Berthelot, 75005 Paris, France

Supporting Information

**ABSTRACT:** The active site of [FeFe] hydrogenase contains a catalytic binuclear iron subsite coordinated by $CN^-$ and CO ligands as well as a unique azadithiolate ($adt^{2-}$) bridging ligand. It has been established that this binuclear cofactor is synthesized and assembled by three maturation proteins HydE, -F, and -G. By means of in vitro maturation in the presence of $^{15}N$- and $^{13}C$-labeled tyrosine it has been shown that the $CN^-$ and CO ligands originate from tyrosine. The source of the bridging $adt^{2-}$ ligand, however, remains unknown. In order to identify the nitrogen of the bridging amine using HYSCORE spectroscopy and distinguish its spectroscopic signature from that of the $CN^-$ nitrogens, we studied three isotope-labeled variants of the H-cluster ($^{15}N$-$adt^{2-}$/$C^{14}N^-$, $^{15}N$-$adt^{2-}$/$C^{15}N^-$, and $^{14}N$-$adt^{2-}$/$C^{15}N^-$) and extracted accurate values of the hyperfine and quadrupole couplings of both $CN^-$ and $adt^{2-}$ nitrogens. This will allow an evaluation of isotopologues of the H-cluster generated by in vitro bioassembly in the presence of various $^{15}N$-labeled potential precursors as possible sources of the bridging ligand.

Hydrogenases catalyze the reversible formation and oxidation of molecular hydrogen.[1,2] In [FeFe] hydrogenases, a binuclear iron cofactor coordinated by CO and $CN^-$ ligands and featuring an open coordination site has been identified as the catalytic center.[3] This [2Fe] subsite is connected through a bridging cysteine to a [4Fe-4S] cluster, forming the so-called "H-cluster" (Figure 1). Of particular importance is the bridging 2-azapropane-1,3-dithiolate (or azadithiolate, $adt^{2-}$) ligand connecting the two irons in the $[2Fe]_H$ subsite. The central amine is believed to play a key role as a proton shuttle in the catalytic cycle.[4−6] It has recently been shown that the binuclear part of the H-cluster can be reconstituted inside the unmaturated form of the [FeFe] hydrogenase, which contains only the $[4Fe\text{-}4S]_H$ subcluster, using a synthetic binuclear precursor $[Fe_2(adt)(CO)_4(CN)_2]^{2-}$.[7,8] It is believed that a similar assembly process occurs in vivo, where the binuclear subsite is first synthesized by the radical *S*-adenosylmethionine maturation proteins HydE and HydG and subsequently inserted into the unmaturated [FeFe] hydrogenase using the third maturation protein HydF.[3,9] The groups of Broderick and Roach demonstrated that the $CN^-$ and CO ligands of $[2Fe]_H$ are synthesized from the substrate tyrosine by HydG.[9] Subsequent extensive electron paramagnetic resonance (EPR) and Fourier transform IR experiments by Britt and Swartz using $^{15}N/^{13}C$-labeled tyrosine and $^{57}Fe$-labeled HydG revealed that the first step in $[2Fe]_H$ synthesis is the formation of a cysteine-coordinated $Fe(CO)_2(CN)$ synthon on HydG.[10−13] The origin of the $adt^{2-}$ ligand, however, remains a mystery. It is speculated that HydE is involved in the synthesis of $adt^{2-}$ and the further assembly of the $[2Fe]_H$ precursor using an as-yet unknown substrate. In order to identify this substrate, an elegant strategy would be to $^{15}N$-label potential candidates and analyze the electron spin echo envelope modulation (ESEEM) signals of the bioassembled H-cluster, looking for a specific $^{15}N$ signal of the $^{15}N$-labeled $adt^{2-}$ ligand. In order to distinguish the $adt^{2-}$ nitrogen signal from the overlapping $CN^-$ signal, we prepared three isotope-labeled variants of the H-cluster ($^{15}N$-$adt^{2-}$/$C^{14}N$, $^{15}N$-$adt^{2-}$/$C^{15}N$, and $^{14}N$-$adt^{2-}$/$C^{15}N$) using the in vitro method that we recently reported[8] and extracted accurate values of the hyperfine and quadrupole couplings of both the $CN^-$ and $adt^{2-}$ nitrogens.

The [FeFe] hydrogenase from *Chlamydomonas reinhardtii* (CrHydA1) was prepared in the active oxidized state ($H_{ox}$) according to previously reported procedures.[5] In this state, the $[2Fe]_H$ subcluster is formally in an $Fe^IFe^{II}$ mixed-valence configuration, but the spin density is highly delocalized over the

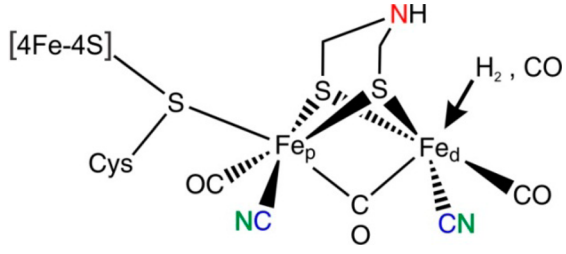


**Figure 1.** Schematic representation of the structure of the H-cluster. The atoms labeled in this work with $^{13}C$ and $^{15}N$ are marked in colors.

**Received:** June 16, 2015
**Published:** September 22, 2015





DOI: 10.1021/jacs.5b06240
J. Am. Chem. Soc. 2015, 137, 12744−12747

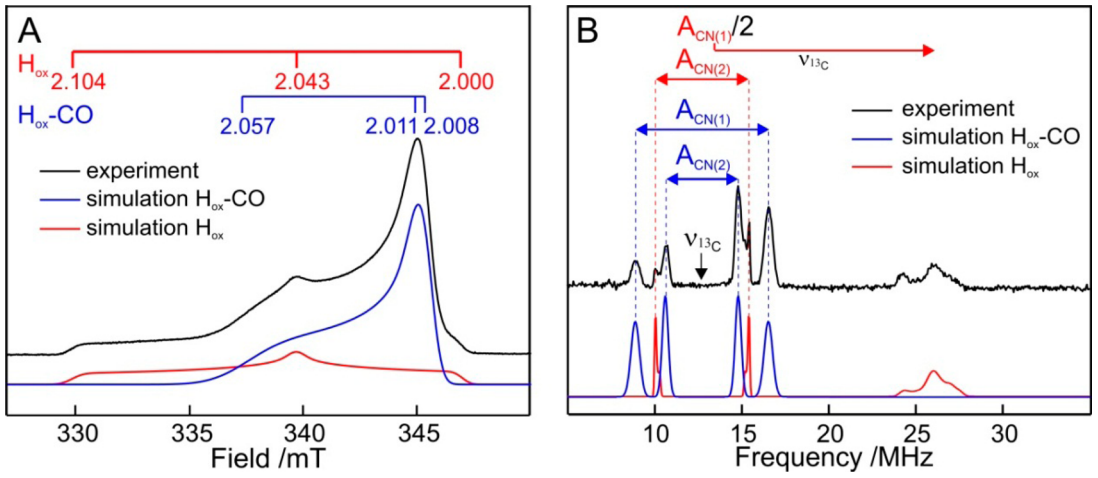


**Figure 2.** (A) X-band free induction decay-detected EPR spectrum of labeled CrHydA1(adt) ($^{15}$N-adt$^{2-}$/C$^{15}$N$^{-}$) together with simulations. The **g** tensor positions for $H_{ox}$ ($g_1$ = 2.104, $g_2$ = 2.043, $g_3$ = 2.000) and $H_{ox}$-CO ($g_1$ = 2.057, $g_2$ = 2.011, $g_3$ = 2.008) are marked above the spectrum. (B) Q-band Davies ENDOR spectrum of $^{13}$C-CN$^{-}$-labeled CrHydA1(adt) recorded at the field position corresponding to the $g_2$ position of $H_{ox}$ together with its simulation. The assignment of the hyperfine splitting is indicated above the figure. The Davies ENDOR spectrum was simulated using the hyperfine parameters indicated in Table S1.

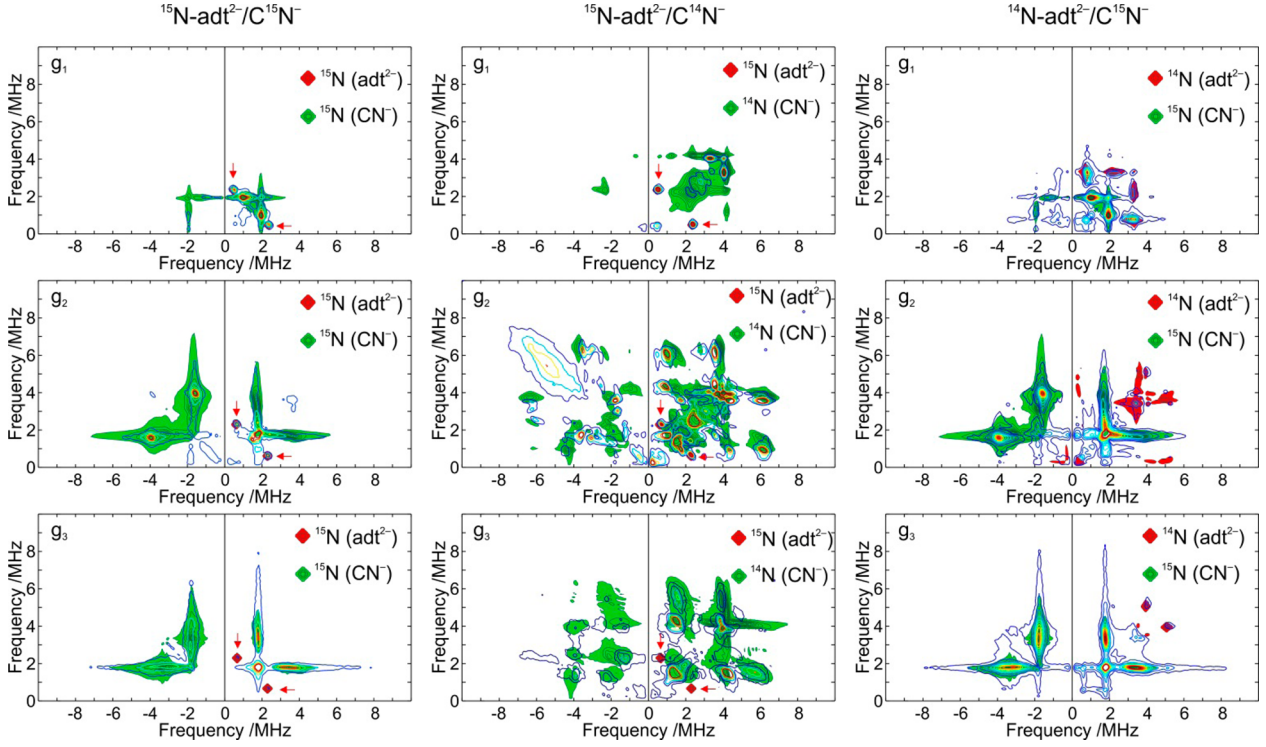


**Figure 3.** X-band HYSCORE spectra (20 K, $\tau$ = 180 ns) recorded at the three canonical positions for CrHydA1(adt) in the $H_{ox}$ state (see Figure 2) with selective isotope-labeling combinations ($^{15}$N-adt$^{2-}$/C$^{15}$N$^{-}$, $^{15}$N-adt$^{2-}$/C$^{14}$N$^{-}$, and $^{14}$N-adt$^{2-}$/C$^{15}$N$^{-}$). All spectra were simulated using parameters from Tables 1 and 2; the simulations for the CN$^{-}$ ligands are presented in green and those for the adt$^{2-}$ ligand in red, superimposed on the experimental results.

iron centers in both the $[2Fe]_H$ subcluster and the $[4Fe\text{-}4S]_H$ subcluster, making it a perfect candidate to observe signals from the CN$^{-}$ and adt$^{2-}$ ligands.[14,15] In practice, preparations of the $H_{ox}$ state are often contaminated with variable contributions from the CO-inhibited state ($H_{ox}$-CO)[14] (in our case ≈ 50%). The EPR signals of $H_{ox}$ and $H_{ox}$-CO overlap (see Figure 2A). In a recent study, we demonstrated that the oxidized CrHydA1(pdt) hybrid (pdt$^{2-}$ = propane-1,3-dithiolate, in which $CH_2$ replaces NH as the head group in the dithiolate bridge) exhibits a pure signal spectroscopically identical to that of the $H_{ox}$ state in CrHydA1(adt).[16] The $^{13}$C hyperfine interaction (HFI) from the two CN$^{-}$ ligands differs by a factor of 5. Scaling the CN$^{-}$ $^{14}$N HFI tensor by the same amount would account for the fact that only one CN$^{-}$ ligand can be observed in $^{15/14}$N hyperfine sublevel correlation spectroscopy (HYSCORE) experiments on oxidized CrHydA1(pdt).[16] As shown in Table S1 and Figure S1, the obtained $^{13}$C hyperfine parameters for oxidized CrHydA1(pdt) and $H_{ox}$(adt) are identical, allowing the assumption that also in $H_{ox}$(adt) only the nitrogen HFI can be detected from one of the CN$^{-}$ ligands.


DOI: 10.1021/jacs.5b06240
J. Am. Chem. Soc. 2015, 137, 12744−12747

Table 1. Principal Values[a] of the $^{15}N$ Hyperfine Tensors of the $adt^{2-}$ and $CN^-$ Ligands of CrHydA1(adt) in the $H_{ox}$ State Compared to Those of Oxidized CrHydA1(pdt)[16]

| | | $A_1$ (MHz) | $A_2$ (MHz) | $A_3$ (MHz) | $A_{iso}$ (MHz) | $\alpha$ (deg) | $\beta$ (deg) | $\gamma$ (deg) |
|---|---|---|---|---|---|---|---|---|
| CrHydA1(adt) in $H_{ox}$ | $adt^{2-}$ | 1.9 (0.1) | 1.6 (0.1) | 1.6 (0.1) | 1.7 | 0 (10) | 0 (10) | 0 (10) |
| | $CN^-$ | −1.3 (0.2) | −1.1 (0.2) | 5.9 (0.2) | 1.2 | 0 (10) | 45 (10) | 90 (10) |
| oxidized CrHydA1(pdt) | $CN^-$ | −1.3 (0.2) | −1.1 (0.2) | 6.2 (0.2) | 1.3 | 0 (10) | 50 (10) | 90 (10) |

[a]The signs of the hyperfine couplings cannot be determined. Numbers in parentheses are uncertainties.

Table 2. Principal Values of the $^{14}N$ Hyperfine and Quadrupole Tensors of the $adt^{2-}$ and $CN^-$ Ligands of CrHydA1(adt) in the $H_{ox}$ State Compared to Those of Oxidized CrHydA1(pdt)[16]

| | | Hyperfine Coupling | | | | | | |
|---|---|---|---|---|---|---|---|---|
| | | $A_1$ (MHz) | $A_2$ (MHz) | $A_3$ (MHz) | $A_{iso}$ (MHz) | $\alpha$ (deg) | $\beta$ (deg) | $\gamma$ (deg) |
| CrHydA1(adt) in $H_{ox}$ | $adt^{2-}$ | 1.35 (0.1) | 1.15 (0.1) | 1.15 (0.1) | 1.2 | 0 (10) | 0 (10) | 0 (10) |
| | $CN^-$ | −0.9 (0.2) | −0.8 (0.2) | 4.2 (0.2) | 0.8 | 0 (10) | 45 (10) | 90 (10) |
| oxidized CrHydA1(pdt) | $CN^-$ | −0.9 (0.2) | −0.8 (0.2) | 4.4 (0.2) | 0.9 | 0 (10) | 50 (10) | 90 (10) |
| | | Quadrupole Coupling | | | | | | |
| | | $K$ (MHz) | $\eta$ | $\alpha$ (deg) | | $\beta$ (deg) | | $\gamma$ (deg) |
| CrHydA1(adt) in $H_{ox}$ | $adt^{2-}$ | 1.23 (0.03) | 0.13 (0.02) | 0 (10) | | 90 (10) | | 0 (10) |
| | $CN^-$ | 0.90 (0.03) | 0.34 (0.02) | 0 (10) | | 119 (10) | | 46 (10) |
| oxidized CrHydA1(pdt) | $CN^-$ | 0.90 (0.03) | 0.34 (0.02) | 0 (10) | | 119 (10) | | 46 (10) |

To estimate the possible contributions of the $CN^-$ ligands in the $H_{ox}$-CO state of CrHydA1(adt) to the HYSCORE spectra of our $H_{ox}$ preparations, we recorded the $^{13}C$ HFI parameters for both $CN^-$ ligands (see Figure S1A). The $CN^-$ $^{13}C$ HFI parameters for both $H_{ox}$ and $H_{ox}$-CO are summarized in Table S1. The magnitude of the $CN^-$ ligand $^{13}C$ HFI closely follows that of the $^{57}Fe$ HFI,[14] indicating that the effective spin density on the binuclear subcluster in the $H_{ox}$-CO state is approximately 5 times smaller than that in the $H_{ox}$ state, as is clearly visible in the Davies electron−nuclear double resonance (ENDOR) spectrum presented in Figure 2B. The group of Britt essentially came to the same conclusions when studying the $CN^-$ HYSCORE and ENDOR signals from [FeFe] hydrogenase from *Clostridium pasteurianum* obtained through in vitro maturation using $^{13}C$- and $^{15}N$-labeled tyrosine.[11] As a final check, we prepared the pure $H_{ox}$-CO state with $^{15}N$-labeled $adt^{2-}$. The resulting HYSCORE spectra (shown in Figures S2−S4) display only minor $C^{14}N$ contributions that do not interfere with the $H_{ox}$ HYSCORE signals.

In Figure 3 the X-band HYSCORE spectra of CrHydA1(adt) $H_{ox}$ selectively labeled as $^{15}N$-$adt^{2-}/C^{15}N^-$, $^{15}N$-$adt^{2-}/C^{14}N^-$, and $^{14}N$-$adt^{2-}/C^{15}N^-$ are presented. As expected, the HYSCORE spectra of the doubly labeled $H_{ox}$ state ($^{15}N$-$adt^{2-}/C^{15}N^-$) (see the first column of Figure 3) are relatively simple and easy to interpret (see Table 1). In particular, the HFI of $^{15}N$-$adt^{2-}$ is virtually isotropic ($A_{iso}$ = 1.7 MHz). Since its hyperfine coupling (1.7 MHz) is less than twice the $^{15}N$ Zeeman frequency at the X-band (≈ 3 MHz), the HYSCORE correlation signals show up in the (++) quadrant (i.e., the right-hand side of the two-dimensional pattern).[17] Because of the isotropic nature of the HFI, the $^{15}N$ $adt^{2-}$ correlation signals recorded at $g_1$, $g_2$, and $g_3$ are virtually identical and show very sharp and well-defined peaks (indicated with the arrows in Figure 3). These features can be recognized even in the HYSCORE spectra of the partially labeled active site ($^{15}N$-$adt^{2-}/C^{14}N^-$) (see the second column of Figure 3). This greatly facilitates the identification of the specific $^{15}N$ signal of the bridging $adt^{2-}$ ligand. The HFI tensor of the $CN^-$ ligand is much more anisotropic and not aligned with the **g** tensor. Because one hyperfine component has a value larger than twice the $^{15}N$ Larmor frequency at the X-band (≈ 3 MHz), the correlation patterns become very broad and also have contributions in the (+−) quadrant (i.e., the left-hand part of the HYSCORE spectrum in Figure 3). The $^{15}N$ $CN^-$ HFI tensor is virtually identical to that found for oxidized CrHydA1(pdt).[16] The $^{15}N$ HFI parameters can now be used as a starting point for the simulation of the $^{15}N$-$adt^{2-}/C^{14}N^-$ and $^{14}N$-$adt^{2-}/C^{15}N^-$ HYSCORE signals (see Table 2). The obtained nuclear quadrupole interaction parameters are summarized in Table 2. It can be easily verified that the $^{14}N$ coupling parameters for the $CN^-$ ligand in CrHydA1(adt) and oxidized CrHydA1(pdt) are virtually identical. This suggests that the central atom of the bridging dithiolate has only a minor effect on the electronic structure of the iron core.

When we compare the $^{14}N$ HFI and quadrupole interaction parameters of both the $CN^-$ and $adt^{2-}$ ligands with those previously estimated for the [FeFe] hydrogenase from *Desulfovibrio desulfuricans* (DdH)[4] (see Table S2), we must conclude that the extracted HFI parameters for DdH were inaccurate. However, the HYSCORE patterns turn out to be much more sensitive to the quadrupole parameters than to the relatively small HFI. This could explain why the quadrupole parameters of DdH (ref 4) and CrHydA1 (current study) came out the same within experimental error. The assignment of these quadrupole parameters to a bridging amine and a $CN^-$ ligand formed the basis for the identification of the $adt^{2-}$ moiety as part of the H-cluster.[4,18] Furthermore, it should be noted that the Q-band $^{14}N$ HYSCORE spectra (Figure S2) show a strong overlap of the spectral features for the $adt^{2-}$ and $CN^-$ ligands. Therefore, the Q-band HYSCORE spectra do not contribute much to the fitting of the $^{14}N$ magnetic parameters of CrHydA1(adt) in the $H_{ox}$ state. In fact, it turns out that the Q-band HYSCORE spectral features originally assigned to the $^{14}N$ signal of Lys237 in our DdH study[14] are actually part of the $CN^{-14}N$ signal (see Figure S2).

In conclusion, we have demonstrated that the X-band $^{15}N$-$adt^{2-}$ HYSCORE features of CrHydA1($^{15}N$-adt) are very well defined and easy to identify (see Figure 3). We thus have presented here the very first and unique probe to monitor the presence of $^{15}N$-labeled $adt^{2-}$ within the active site of [FeFe]


DOI: 10.1021/jacs.5b06240
J. Am. Chem. Soc. 2015, 137, 12744−12747

hydrogenase. Our data should provide a solid basis to screen $^{15}$N-labeled potential precursors of adt$^{2-}$ using the in vitro cell-free [FeFe] hydrogenase maturation methodology developed by Swartz and co-workers based on the combination of individually expressed maturases HydE, HydG, and HydF with unmaturated [FeFe] hydrogenase. The discovery of the precursor of adt$^{2-}$, the missing link of the [FeFe] hydrogenase maturation process, will hopefully allow a complete description of this fascinating biosynthetic pathway.

## ■ ASSOCIATED CONTENT

### Supporting Information

The Supporting Information is available free of charge on the ACS Publications website at DOI: 10.1021/jacs.5b06240.

Materials and Methods, $^{13}$C interaction of the CN$^-$ ligands, HYSCORE spectra of CrHydA1(adt) in the $H_{ox}$ state, $^{14/15}$N interaction of the adt$^{2-}$ and CN$^-$ ligands, and comparison of HYSCORE spectra of DdH and CrHydA1 (PDF)

## ■ AUTHOR INFORMATION


### Corresponding Authors

*wolfgang.lubitz@cec.mpg.de
*edward.reijerse@cec.mpg.de

### Present Address

‖T.R.S.: Energy Materials Laboratory, University of East Anglia, Norwich Research Park, Norwich, Norfolk NR4 7TJ, U.K.


### Notes

The authors declare no competing financial interest.

## ■ ACKNOWLEDGMENTS

This work was supported by the Max Planck Society and the DFG (DIP Project LU 315/17-1). V.A., S.R., and T.R.S. acknowledge the French National Research Agency (Labex Program, ARCANE, ANR-11-LABX-0003-01) and the Bioenergy Program of the Life Science Division of CEA. M.F. acknowledges the Fondation de l'Orangerie for individual philanthropy and its donors as well as the French State Program "Investissements d"Avenir' (Grants "LABEX DYNAMO", ANR-11-LABX-0011).

## ■ REFERENCES


(1) Cammack, R.; Frey, M.; Robson, R. *Hydrogen as a Fuel: Learning from Nature*; Taylor & Francis: London, 2001.
(2) Vignais, P. M.; Billoud, B. *Chem. Rev.* **2007**, *107*, 4206.
(3) Lubitz, W.; Ogata, H.; Rüdiger, O.; Reijerse, E. *Chem. Rev.* **2014**, *114*, 4081.
(4) Silakov, A.; Wenk, B.; Reijerse, E.; Lubitz, W. *Phys. Chem. Chem. Phys.* **2009**, *11*, 6592.
(5) Adamska, A.; Silakov, A.; Lambertz, C.; Rüdiger, O.; Happe, T.; Reijerse, E.; Lubitz, W. *Angew. Chem., Int. Ed.* **2012**, *51*, 11458.
(6) Nicolet, Y.; de Lacey, A. L.; Vernede, X.; Fernandez, V. M.; Hatchikian, E. C.; Fontecilla-Camps, J. C. *J. Am. Chem. Soc.* **2001**, *123*, 1596.
(7) Berggren, G.; Adamska, A.; Lambertz, C.; Simmons, T.; Esselborn, J.; Atta, M.; Gambarelli, S.; Mouesca, J. M.; Reijerse, E.; Lubitz, W.; Happe, T.; Artero, V.; Fontecave, M. *Nature* **2013**, *499*, 66.
(8) Esselborn, J.; Lambertz, C.; Adamska-Venkatesh, A.; Simmons, T.; Berggren, G.; Noth, J.; Siebel, J.; Hemschemeier, A.; Artero, V.; Reijerse, E.; Fontecave, M.; Lubitz, W.; Happe, T. *Nat. Chem. Biol.* **2013**, *9*, 607.
(9) Shepard, E. M.; Mus, F.; Betz, J. N.; Byer, A. S.; Duffus, B. R.; Peters, J. W.; Broderick, J. B. *Biochemistry* **2014**, *53*, 4090.
(10) Kuchenreuther, J. M.; Myers, W. K.; Stich, T. A.; George, S. J.; NejatyJahromy, Y.; Swartz, J. R.; Britt, R. D. *Science* **2013**, *342*, 472.
(11) Myers, W. K.; Stich, T. A.; Suess, D. L. M.; Kuchenreuther, J. M.; Swartz, J. R.; Britt, R. D. *J. Am. Chem. Soc.* **2014**, *136*, 12237.
(12) Kuchenreuther, J. M.; Myers, W. K.; Suess, D. L. M.; Stich, T. A.; Pelmenschikov, V.; Shiigi, S. A.; Cramer, S. P.; Swartz, J. R.; Britt, R. D.; George, S. J. *Science* **2014**, *343*, 424.
(13) Suess, D. L. M.; Bürstel, I.; De La Paz, L.; Kuchenreuther, J. M.; Pham, C. C.; Cramer, S. P.; Swartz, J. R.; Britt, R. D. *Proc. Natl. Acad. Sci. U. S. A.* **2015**, *112*, 11455.
(14) Silakov, A.; Reijerse, E. J.; Albracht, S. P. J.; Hatchikian, E. C.; Lubitz, W. *J. Am. Chem. Soc.* **2007**, *129*, 11447.
(15) Silakov, A.; Reijerse, E. J.; Lubitz, W. *Eur. J. Inorg. Chem.* **2011**, 1056.
(16) Adamska-Venkatesh, A.; Simmons, T. R.; Siebel, J. F.; Artero, V.; Fontecave, M.; Reijerse, E.; Lubitz, W. *Phys. Chem. Chem. Phys.* **2015**, *17*, 5421.
(17) Schweiger, A.; Jeschke, G. *Principles of Pulse Electron Paramagnetic Resonance*; Oxford University Press: Oxford, U.K., 2001.
(18) Erdem, O. F.; Schwartz, L.; Stein, M.; Silakov, A.; Kaur-Ghumaan, S.; Huang, P.; Ott, S.; Reijerse, E. J.; Lubitz, W. *Angew. Chem., Int. Ed.* **2011**, *50*, 1439.




DOI: 10.1021/jacs.5b06240
*J. Am. Chem. Soc.* 2015, 137, 12744−12747